Influence of Calcium Nitrate and Sodium Hydroxide on Carbonation-Induced Steel Corrosion in Concrete

Matteo Stefanoni,[‡,] Ueli Angst,[*] and Bernhard Elsener[*,**]*

Recent developments in concrete technology, together with sustainability concerns and requirements related to digital concrete fabrication technologies, lead to increased usage of chemical admixtures in order to achieve the needed concrete performance. However, the consequences that these compounds may have for the long-term durability are unknown, particularly concerning steel reinforcement corrosion. Here, we study the effect of NaOH and $Ca(NO_3)_2$ as common examples of a hydration activator and accelerator, respectively. It is found that both admixtures considerably increase the steel corrosion rate in carbonated concrete (by up to a factor of 20). Corrosion tests in mortar as well as in aqueous solutions, together with porosity measurements of the mortars, provided evidence that the impact of the admixtures can be mainly found in modifying the electrochemistry, that is, by introducing an additional reduction reaction or by a catalyzing effect. An estimation revealed that at usual dosages, these adverse effects will prevail for a substantial portion of the design service life of a structure, as these species will not be consumed during decades.

KEY WORDS: carbon steel, corrosion rate, general corrosion, nitrates, porosity, steel-reinforced concrete

INTRODUCTION

Activation and controlled acceleration of setting and hardening of cementitious materials is becoming increasingly important because of very different, but yet complementary reasons. The cement industry, after relying for decades on traditional methods, is now facing the beginning of a revolution. On one side, the international efforts toward a more sustainable future[1] are demanding a substantial reduction of the environmental impact of the cement industry (nowadays responsible for ca. 8% of manmade CO_2 emissions), resulting in important modifications of the binder composition.[2-5] On the other, the recent and abrupt interest in digital fabrication techniques applied to the construction industry requires drastic changes in the processing of cementitious materials, strongly affecting mix design and hardening requirements.[6-7] Although, the use of alkali-activated materials has been known since the 1930s,[8] the topic has gained large attention recently, because of the possibility to activate a wide variety of materials, which can be used to replace the poorly sustainable ordinary Portland cement.[5,9-10] The main alkali-activated materials used worldwide are furnace slag and fly ash; but, on a smaller scale, many others are used and studied,[10] depending on local availability. The common denominator of these materials is the need of the hardening process to be activated by a highly alkaline environment, which can be obtained by the use of alkaline compounds directly added in the mix design (such as NaOH and many others).[10] The use of accelerators has been necessary in the past for applications such as casting in cold environments and others.[11-13] In case of alkali-activated binders they are needed to improve the early age strength and satisfy the requirements of the construction companies. Furthermore, the newborn interest in digital fabrication with concrete (such as 3D printing[6] and dynamic casting technologies[14]) requires a reliable control of hydration time and hardening properties, which is possible only thanks to the use of accelerators.[7] This family of admixtures was once only composed by one member, calcium chloride, which is no longer an option due to severe corrosion hazards in steel-reinforced concrete.[13] One of the most common alternatives is calcium nitrate, even though it is less efficient.[13] Today, most suppliers of concrete admixtures offer calcium nitrate-based accelerators.

When it comes to possible influence of these compounds (activators and accelerators), with respect to steel reinforcement corrosion, the use of NaOH has never been taken into account as an independent possible influencing parameter of rebars corrosion, at the best of our knowledge. On the other hand, calcium nitrate has been found to be an effective inhibitor for chloride-induced corrosion,[15-16] earning the title of "multifunctional admixture" for concrete.[17] Nevertheless, the possible impact of both activators and accelerators should be evaluated in terms of carbonation-induced corrosion. This is because the majority of the new environmentally friendly binders are characterized by a lower resistance to carbonation[18-19] and because digitally fabricated structures, predominantly used in the context of architecture, likely are mainly exposed to carbonation environments.[20] The use of calcium nitrate might be able to increase the carbonation resistance thanks to a pore structure refinement. However, this may only occur under some conditions, but not under others, as the

Submitted for publication: October 25, 2018. Revised and accepted: March 16, 2019. Preprint available online: March 18, 2019, https://doi.org/10.5006/3085.
‡ Corresponding author. E-mail: matteost@ethz.ch.
* ETH Zurich, Institute for Building Materials, Stefano-Franscini-Platz 3, Zurich CH-8093, Switzerland.
** University of Cagliari, Department of Chemical and Geological Science, I-09100 Monserrato (CA), Italy.

ISSN 0010-9312 (print), 1938-159X (online)

admixture performances seem to depend largely on the binder composition.[21]

In this publication the effect of NaOH and $Ca(NO_3)_2$ on the corrosion rate of steel is investigated in carbonated mortars, realized with a highly substituted blended cement. The results show that both admixtures can have a significant impact, which can be explained by different contributions lying in the specific chemical reactivity and in the impact on the pore solution chemistry. The overall behavior suggests that the use of these compounds should be carefully evaluated, also with respect to their impact on the long-term durability.

EXPERIMENTAL PROCEDURES

2.1 | Test Sample Specifications

Mortar samples (dimension 80 mm^3 × 80 mm^3 × 6 mm^3) were cast with embedded carbon steel (St 37) wires (diameter = 0.5 mm) serving as working electrodes, a stainless steel grid (10 mm^3 × 100 mm^3 × 1 mm^3), to be used as counter electrode, and an embedded Ag/AgCl sensor acting as reference electrode for the electrochemical tests.[22-23]

2.2 | Mix Design

A new blended binder (from now on referred to as new binder (NB) has been used, as activators and accelerators are primarily used to guarantee the early age performances of new binders that are otherwise slowly reactive. The present one is composed by: 50% Portland cement, 20% limestone powder, 20% burnt oil shale, and 10% furnace slag. Ordinary Portland cement (CEM I 52.5) was used as a reference material, without addition of any activator or accelerator. The mix design was chosen to allow the best workability, while maintaining a high stability of the cementitious suspension. The w/b ratio was 0.5, the sand/binder ratio was 2, and the sand had a maximum particle diameter of 1 mm. A polycarboxylate ether superplasticizer with defoaming agent was added in the amount of 0.2% by weight of binder, in order to increase the fluidity and thus permitting filling the molds. The specimens were demolded after 1 day and cured at 95% RH for 7 days before being carbonated.

2.3 | Activator and Accelerator

The alkaline activator used in this study is NaOH, while the accelerator is $Ca(NO_3)_2$. In the different series tested, they were added to the mixing water in the following amounts with respect to the binder weight:

- NaOH, 1%;
- NaOH, 5%;
- $Ca(NO_3)_2$, 1%;
- $Ca(NO_3)_2$, 5%;
- NaOH, 1%; $Ca(NO_3)_2$, 1%.

Common dosage of $Ca(NO_3)_2$ is up to 4% by weight of binder, depending on the expected performance.[17] For NaOH, the dosage depends not just on performance, but also on the binder composition. In the case of slag cement (slag content up to 95%), amounts up to 10% by weight of slag are used;[24] the dosage is usually reduced when the fraction of CEM I in the binder is increased.

2.4 | Carbonation Procedure

The samples were carbonated in a carbonation chamber at 20°C, 57% relative humidity, and 4% CO_2 concentration. The time required for complete carbonation was 7 day for CEM I samples, and less than 3 day for all NB samples. These results were obtained by the phenolphthalein test[25] on companion samples, prior to the experimental study. To ensure complete carbonation of the samples used for the present study, a safety extra-time in the carbonation chamber was applied: the NB mortars were carbonated for 2 weeks, while 3 weeks was used for the CEM I mortars.

2.5 | Exposure Conditions

After carbonation, the samples were studied in different exposure conditions of controlled and constant environments: 81% RH, 95% RH, and 99% RH at a temperature of 20°C. The relative humidity was controlled by means of either climatic conditioning rooms (95% RH) or of saturated Ammonium Sulfate solution (81% RH) or ultrapure water (99% RH), taking care no water condensation would take place in the container by keeping the temperature constant.

2.6 | Time to Equilibration

Monitoring of the mass of the samples showed a weight equilibration for all the different samples, at a constant relative humidity, after 1 to 2 weeks. The measurements of corrosion rate started after minimum 2 months of exposure at a constant relative humidity, once stable conditions were achieved.

2.7 | Electrochemical Tests

All the electrochemical tests were performed using a potentiostat Metrohm Autolab PGSTAT30[†]. The embedded Ag/AgCl sensor was always used as reference electrode and its reference potential was checked by means of an external Ag/AgCl reference electrode. One carbon steel wire was used as working electrode and the stainless steel grid was used as counter electrode. The measurements were repeated over time for each exposure condition. The measurements described below have been performed on two different mortar specimens per each mix and three wires per specimen. This gives six different tested wires per mix.

Corrosion rate: the instantaneous corrosion current density was determined by polarization resistance measurements.[26] The polarization resistance $R_{p'}$ of the single steel wires was measured at ±10 mV around the open circuit potential with a scan rate of 0.1 mV/s. The IR-drop in the mortar was taken into account indirectly. Impedance measurements (see below) were performed right before each polarization resistance test, and the obtained ohmic resistance R_Ω was subtracted from the total resistance $R_{p'}$ to get the IR drop-free polarization resistance values R_p.

The corrosion rate, i_{corr}, was then calculated using the following equation:

$$i_{corr} = B/R_p \quad (1)$$

where B is a parameter depending on the electrochemical properties of the considered system; for iron in actively corroding state a value of 26 mV is commonly used.[27-28] A source of error could come from the fact that, as shown later in the Discussion section, the cathodic reactions involved in the corrosion process are changing depending on the samples. An estimation of the magnitude of the possible error has been performed on the basis of the expression of the B parameter in Andrade and Alonso[27] and Equations (4) through (7) of this work. It results that, theoretically, B could become up to 25% lower in a system

[†] Trade name.

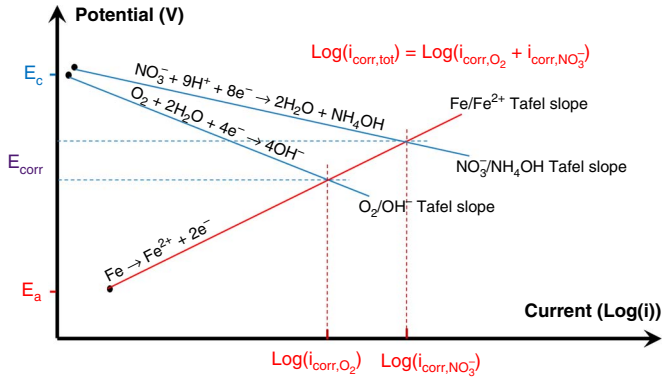

FIGURE 1. *Evans diagram representing the electrochemical system of iron corrosion in presence of O_2 and NO_3^- in conditions (pH) where steel passivation is not possible. The high number of electrons that can be delivered to the nitrogen atoms can strongly increase the anodic iron dissolution rate. The final corrosion rate is equal to the sum of the two cathodic processes.*

such as the one depicted in Figure 1, with the additional reduction of nitrates. Finally, the value of B has been maintained equal for all measurements because of the impossibility of reliably defining the variation for each specific system and because the possible out coming error is estimated in the order of the standard deviation of our measurements.[28]

Ohmic resistance (R_Ω) in the same electrode configuration as for the polarization resistance tests, the electrical resistance was measured by means of electrochemical impedance spectroscopy (50 frequencies logarithmically distributed between 10^5 and 1 Hz, voltage amplitude = 10 mV). The value of ohmic resistance R_Ω was extrapolated by fitting of the first semicircle appearing in the Nyquist plot and considering the value first intercepted on the real impedance axis.

Two specimens per each mix design were produced and three wires per specimen were used for corrosion rate measurements; therefore, each value reported in this work is an average of six measurements.

2.8 | Mercury Intrusion Porosity Tests

The ***mercury intrusion porosity*** (MIP) tests were performed with a porosimeter from Thermoscience (Pascal 140/440). Plain mortar samples were produced in the same way described above, but without embedded electrodes. After carbonation the samples were saturated with isopropanol in order to remove the water and preserve the microstructure; the isopropanol was replaced every day for one week. The samples were then dried into a desiccator with silica gel and under vacuum. Five small mortar pieces of similar size and shape were cut at the moment of the test, which started from a pressure of 0.012 MPa up to 400 MPa which allows mercury intrusion in pores down to theoretically 2 nm radius (assuming a contact angle of 140°). Repetitions were performed and showed good reproducibility.

2.9 | Pore Solution Composition

Inductively coupled plasma optical emission spectrometry (ICP-OES) pore solution elemental analysis of carbonated samples of CEM I, NB, and NB+1%NaOH was performed to check the ionic content and try to better understand the influence of NaOH addition on the final steel corrosion rate. Pore solution was extracted from samples realized with the same mix design, curing, and carbonation conditions as the specimens prepared for electrochemical and porosity tests. Cylinders of 5 cm diameter were prepared for each mix, using the same mix designs as described in the "Mix Design" section. After demolding, the cylinders were cut in slices 0.5 cm to 1 cm thick, which were cured for 7 days. Afterward, the slices were carbonated as in the "Carbonation Procedure" section and finally left at 99% RH for 2 months and occasionally sprayed with ultrapure water, in order to achieve good water saturation. The extraction was performed on 10 slices per mix type, by means of a hydraulic press applying a pressure up to 300 MPa for a time between 30 min and 3 h. The so extracted solutions were than analyzed by ICP-OES and the elements Na, K, Ca, and S were quantified.[29]

Table 1. *Pore Solution Composition of the Mixes CEM I, NB, and NB +1% NaOH*[(A)]

Mix	Ca (M)	K (M)	Na (M)	S (M)
CEM I	0.0186	0.0151	0.0056	0.0065
NB	0.0205	0.0093	0.0057	0.0083
NB +1% NaOH	0.0149	0.0081	0.0751	0.0206

[(A)] Average values for three repetitions, whose resulting standard deviation is ±1%.

Tests in Simulated Carbonated Concrete Pore Solution

In order to measure the impact of specific chemical species on the corrosion rate of carbon steel, the results of pore solution composition described in the previous section was used to prepare solutions with similar composition (see Table 1). The reference solution contained:

- $Ca(OH)_2$, saturated;
- KOH, 0.01 M;
- $CaSO_4$, 0.007 M.

The solution (pH ca. 13) was carbonated by bubbling CO_2, until pH ca. 8 (resulting solution, from now on called "R").

In order to clarify the influence of sulfate and nitrate ions on the steel corrosion rate, the following solutions were prepared:

- R (Reference);
- S, composed of R + 0.013 M Na_2SO_4, to check the influence of sulphate ions;
- N, composed of R + 0.0065 M $Ca(NO_3)_2$, that is $[NO_3^-]$ = 0.013 M, to check the influence of nitrate ions;
- S-N, composed of R + 0.013 M Na_2SO_4 + 0.0065 M Ca $(NO_3)_2$, to check the combined effect.

For solution S, the added amount (0.013 M) was chosen in order to match the total sulphate content as found by ICP-OES, in the solution extracted from the mix NB +1% NaOH.

The corrosion rate of the same type of wires embedded in the mortar samples (see the "Test Sample Specifications" section) was measured upon immersion of the wires in these solution, by means of the same electrochemical methods described in the Section "Electrochemical Tests."

RESULTS

3.1 | Corrosion Rate in Mortar

Table 2 and Figure 2 report the average corrosion rate and standard deviation measured for all mix designs used in this

Table 2. *Steel Corrosion Rate for the Different Mixes*[A]

	Mix	Exposure Condition		
		81% RH	95% RH	99% RH
Corrosion Rate (μA/cm^2)	CEM I	$9.42 \times 10^{-3} \pm 2.8 \times 10^{-3}$	$2.85 \times 10^{-2} \pm 8.8 \times 10^{-4}$	$7.88 \times 10^{-2} \pm 9.0 \times 10^{-3}$
	NB	$2.70 \times 10^{-2} \pm 1.8 \times 10^{-3}$	$1.07 \times 10^{-1} \pm 1.5 \times 10^{-2}$	$2.24 \times 10^{-1} \pm 2.2 \times 10^{-2}$
	NB + 1% NaOH	$7.00 \times 10^{-2} \pm 1.9 \times 10^{-2}$	$2.50 \times 10^{-1} \pm 9.1 \times 10^{-2}$	$7.46 \times 10^{-1} \pm 7.1 \times 10^{-2}$
	NB + 1% $Ca(NO_3)_2$	$1.20 \times 10^{-1} \pm 5.0 \times 10^{-3}$	$4.44 \times 10^{-1} \pm 7.6 \times 10^{-2}$	$4.35 \times 10^{-1} \pm 2.6 \times 10^{-2}$
	NB + 1% NaOH $Ca(NO_3)_2$	$2.12 \times 10^{-1} \pm 7.1 \times 10^{-3}$	$7.83 \times 10^{-1} \pm 5.3 \times 10^{-2}$	$1.26 \times 10^{-0} \pm 2.3 \times 10^{-1}$
	NB + 5% NaOH	$3.10 \times 10^{-1} \pm 5.1 \times 10^{-2}$	$1.98 \times 10^{-0} \pm 4.2 \times 10^{-1}$	$5.70 \times 10^{-0} \pm 3.1 \times 10^{-1}$
	NB + 5% $Ca(NO_3)_2$	$3.64 \times 10^{-1} \pm 4.5 \times 10^{-2}$	$9.24 \times 10^{-1} \pm 7.1 \times 10^{-2}$	$2.49 \times 10^{-0} \pm 7.1 \times 10^{-1}$

[A] Average values and standard deviations for the measurements of six steel wires per mix.

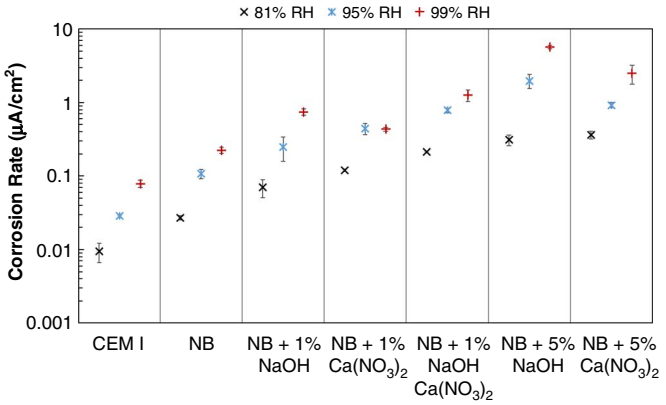

FIGURE 2. *Corrosion rate values (markers = average values of 6 steel wires, whiskers = standard deviations) of 0.5 w/b ratio mortars of CEM I and NB without and with addition of different admixtures and in different amounts.*

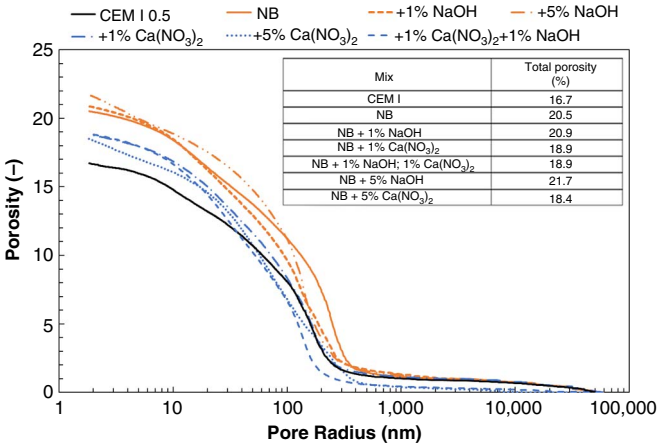

FIGURE 3. *Cumulative porosity curves of the tested samples. The total porosity of each mix is reported.*

study. In agreement with literature, the corrosion rate increases with higher relative humidity.[30-31] The mix NB shows steel corrosion rate values ca. three times higher than CEM I, in line with other data for steel corrosion in low-clinker binders.[30-31] Whenever either NaOH or $Ca(NO_3)_2$ was added, a further increase of corrosion rate has been measured, depending on type and amount of admixture. The addition of 1% of either admixture caused an increase in corrosion rate of approximately a factor 3 to 4. When both NaOH and $Ca(NO_3)_2$ are used at 1%, in the same mix, the effect of the admixtures seems to be additive, leading to a corrosion rate increase of a factor ca. 7, with respect to the bare NB mix. Rising up the admixtures concentration to 5%, the corrosion rate becomes ca. 20 times higher with NaOH and ca. 11 times higher with the addition of Ca $(NO_3)_2$, always with respect to NB. It can also be noticed that in the case of 1% addition of $Ca(NO_3)_2$ there is no further increase in the corrosion rate from 95% to 99% RH; this behavior is not noticed in any other mix (Figure 2).

3.2 | Porosity

The mercury intrusion porosimetry of the carbonated mortars shows that the mortar manufactured with CEM I has the most dense microstructure (Figure 3). Compared to it, the NB specimen presents a 20% higher total porosity. The addition of NaOH does not seem to substantially influence the total porosity, even though it has an impact on the pore size distribution, which shifts toward smaller pores. When $Ca(NO_3)_2$ was used, the final total porosity markedly decreased of ca. 10%, regardless of the concentration. Finally, the combined addition of both admixtures led to a total porosity in line with $Ca(NO_3)_2$ addition and to a shift in the pore size distribution to smaller dimensions (Figure 3).

3.3 | Pore Solution

The analysis of pore solution of carbonated samples (Table 1) revealed that the composition for CEM I and NB is essentially the same, whereas the use of NaOH leads to big differences in the concentration of sodium and sulfur. Na concentration increases by a factor 10, while S goes up by almost a factor of 3 (Table 1). Sulfur, in cement pore solutions, is usually indicative of the presence of SO_4^{2-} ions.

3.4 | Corrosion Rate in Simulated Carbonated Concrete Pore Solution

The results from tests in a solution showed that there is indeed an influence of sulphate and nitrate ions on the steel dissolution rate. Table 3 summarizes the measured corrosion rates, obtained from three steel wires per each simulated solution. The addition of Na_2SO_4 led to ca. 2.5 times higher corrosion rate, while the addition of the same amount of $Ca(NO_3)_2$ increased the steel dissolution only by a factor ca. 1.6. Finally, the solution

Table 3. *Corrosion Rate Values (Average on Three Samples) and Standard Deviation of Steel Wires Immersed in the Solutions Described in Section "Tests in Simulated Carbonated Concrete Pore Solution"*

Solution	Corrosion Rate (μA/cm^2)
R	3.76±0.43
S	9.56±0.53
N	5.93±1.14
S-N	10.86±0.73

containing both chemicals (S-N) showed an increase of corrosion rate of ca. 2.8 times, with respect to the reference (R).

DISCUSSION

The baseline difference between Portland cement mortar (CEM I) and the low-clinker binder mortar (NB) is in agreement with previously reported data, where low-clinker binders have been compared to Ordinary Portland cement.[30,32] The reason for the increase in corrosion rate might be found in the higher porosity of the carbonated NB mortar (20.5%), compared to the carbonated CEM I mortar (16.7%), as already suggested in Stefanoni et al.[30-31] The increasing effect of admixtures on the corrosion rate cannot be explained by an increased porosity, because the addition of NaOH leads to an almost constant total porosity, while the use of $Ca(NO_3)_2$ even decreases it (Figure 3). The increase in corrosion rate in the presence of the admixtures must thus be related to the electrolyte chemistry, which is also evidenced from the results displayed in Table 3. The admixtures bring different chemical species, which are influencing the final composition of the pore solution electrolyte (Table 1) and the electrochemical system, respectively. Therefore, the effect of $Ca(NO_3)_2$ and NaOH has to be analyzed separately.

4.1 | Effect of Calcium Nitrate ($Ca(NO_3)_2$)

Calcium nitrate has been found, over recent decades, to be an effective inhibitor of chloride-induced corrosion.[15,17] Thus, the here-observed effect of $Ca(NO_3)_2$, that is, the increase in corrosion rate, may seem surprising. However, once the electrochemical interaction of the compound with the steel is considered more closely, the reason for such behavior can be explained.

Steel reinforcement in alkaline concrete (with high pH) is protected by the spontaneous formation of a stable iron oxide film (the passive film).[33] In such situation, chlorides are usually the only threat to the steel, as they can locally break down the passive layer. Nitrate ions (NO_3^-), released by the accelerator admixture, are powerful oxidizing agents (see the section "Electrochemistry of Iron Corrosion in Presence of O_2 and NO_3^-"), which are able to quickly reoxidize the steel surface upon chloride-induced breakdown, thus rebuilding the stable protective layer in alkaline pH. This is the suggested mechanism explaining the corrosion inhibiting nature of calcium nitrate in chloride environments.[15] Moreover, nitrates compete with chloride (and hydroxyl) ions in migrating toward the corroding site, contributing to the repassivation effect.

In carbonated concrete, the pH is lowered to values that do not allow for stability of the passive layer.[33] We suggest that once the passive film is dissolved, the fast iron oxidation caused by the presence of nitrates is not leading to the formation of a protective layer anymore, but to an accelerated corrosion process instead. The iron oxidation promoted by nitrate ions is not a new concept; application of such phenomenon has already been implemented in other fields, such as water purification from nitrate ions by means of iron powder.[34-35]

From an electrochemical point of view, the nitrates act as an additional cathodic reaction, upon which nitrogen (initial oxidation state +5) gets reduced to lower oxidation state, possibly until the formation of molecular nitrogen (N_2, oxidation state 0) or ammonium (NH^{4+}, oxidation state −3)[34-35] (details in the following section). In this work, a nitrate-based compound was used (NO_3^-), not to be confused with nitrite (NO_2^-), which is also known as a corrosion inhibitor.[36] The effect of nitrite species might be similar, as their chemistry is very close to nitrates, but it has not been tested in this experimentation.

As mentioned in the section "Corrosion Rate in Mortar," the behavior of the mix +1% $Ca(NO_3)_2$ is peculiar because, unlike for the other mixes, it does not show any corrosion rate increase going from 95% RH to 99% RH exposure condition. This may be explained by a possible dilution effect of the nitrate ions going to higher moisture contents. It is known that the nitrate ions get bound by the cement hydration phases,[36] therefore, the real concentration of free NO_3^- in the cement pore solution could be lowered down to values that are very dependent on the degree of water saturation. When the calcium nitrate content is increased to 5% in the initial mix, the corrosion rate is again strongly increasing with relative humidity, not showing any dilution effect (Table 2, Figure 2).

4.2 | Electrochemistry of Iron Corrosion in Presence of O_2 and NO_3^-

The dissolution of iron in water is a spontaneous electrochemical process, resulting from the simultaneous occurrence of separate semi reactions. Electrons are released in the oxidation reaction (metal dissolution), and consumed in the reduction reaction. For carbon steel in neutral to moderately alkaline environments (pH 7 to 10), the following electrochemical reactions are usually considered:[33]

Oxidation reaction (dissolution of iron):

$$Fe \rightleftarrows Fe^{2+} + 2e^- \quad (2)$$

Reduction reaction (oxygen reduction):

$$O_2 + 2H_2O + 4e^- \rightleftarrows 4OH^- \quad (3)$$

In order for corrosion to occur, the presence of water as well as dissolved oxygen is required. The two semi reactions must occur at the same overall rate (same number of electrons exchanged by unit of time); the resulting electrochemical redox reaction can be written as:

$$2Fe + O_2 + 2H_2O \rightarrow 2Fe(OH)_2 \quad (4)$$

The initial corrosion product $Fe(OH)_2$ will be further oxidized to Fe_3O_4 or Fe_2O_3.[37-38]

When other oxidizing species are present, such as nitrate ions, additional reduction reactions (e.g., Equations [5] and [6]) can take place and participate in the electrochemical process:[39]

$$NO_3^- + 4H^+ + 3e^- \rightleftarrows 2H_2O + NO \quad (5)$$

$$NO + 5H^+ + 5e^- \rightleftarrows NH_4OH \quad (6)$$

According to the Pourbaix diagram of nitrogen species,[40] the reversible potential for nitrate reduction (Equations [5] and

[6]) is comparable to the one for oxygen reduction (Equation [3]). This means the two species (nitrogen and oxygen) can be stable in concrete, without reacting with each other, until there is the possibility for an anodic process to take place, characterized by a more negative reversible potential. Once the steel embedded in carbonated concrete is depassivated, the two cathodic processes can occur simultaneously and couple with the anodic process of iron dissolution. The combination of two cathodic reactions would increase the rate of anodic dissolution (Figure 1). Also, even though the two cathodic reactions have similar electrochemical potential, the potential amount of electrons exchanged per mole of reacting substance is very different, with $4e^-$ for the oxygen reduction (Equation [3]), vs. $8e^-$ for the full reduction of nitrate to ammonium ions (Equations [5] and [6]). According to the expression of the Tafel slope (Equation [7]), when the number of electrons exchanged increases, the Tafel slope decreases, leading to a much higher increase of current for the same polarization (Figure 1).

$$\text{Tafel slope} = \frac{RT}{\alpha n F} \tag{7}$$

with R gas constant, T temperature, α charge transfer coefficient, n number of electrons exchanged in the reaction, and F Faraday constant.

4.3 | Consumption of NO_3^- Ions

When the cathodic reaction driving the corrosion of steel in carbonated mortar is only the oxygen reduction (Equation [3]), the reactant supply of atmospheric O_2 is infinite in atmospheric exposure. On the other hand, nitrates added to the mix as hydration accelerator are consumed by the cathodic reaction (Equations [5] and [6]). Thus, reacted NO_3^- ions are not replaced, which should lead to a depletion of the reactant over time. A simple electrons balance, based on the measured corrosion rates, may thus allow to roughly estimate the duration of the effect of nitrate ions.

Considering that for NB mix, the cathodic reaction is only performed by O_2 reduction, while, when calcium nitrate is added (mix N), both O_2 and NO_3^- reduction contribute to the cathodic process. From the corrosion rate data (Table 2, Figure 2), the effect of the $Ca(NO_3)_2$ addition on the steel corrosion rate can be estimated. Considering the 95% RH exposure condition:

$$i_{corr,NB} = i_{corr,O_2} = 0.11\ \mu A/cm^2 \tag{8}$$

$$i_{corr,1\%Ca(NO_3)_2} = 0.44\ \mu A/cm^2 \tag{9}$$

The difference between Equations (8) and (9) would hypothetically give the corrosion rate driven by the NO_3^- cathodic reaction (i_{corr,NO_3^-}):

$$i_{corr,+1\%Ca(NO_3)_2} - i_{corr,O_2} = i_{corr,NO_3^-} = 0.33\ \mu A/cm^2 \tag{10}$$

Given the total steel area embedded in one specimen (6.28 cm^2), it means the total corrosion current per specimen is 2.07 μA. Therefore, the total exchanged charge and moles of electrons per unit of time can be calculated.

$$2.07\ \mu A = \frac{2.07 \times 10^{-6}\ C/s}{1.6 \times 10^{-19} C/e^-} = 1.3 \times 10^{13} \frac{e^-}{s} = 2.2 \times 10^{-11} \frac{mol(e^-)}{s} \tag{11}$$

The calculated moles of NO_3^-, in one mortar specimen (NB + 1% $Ca(NO_3)_2$) is

$$NO_3^- = 2.6 \times 10^{-3}\ mol \tag{12}$$

Assuming that all of this is available for reaction, we can compute the time it would take to consume all the nitrate ions (t) can be estimated:

$$t = \frac{2.1 \times 10^{-2}\ mol(e^-)}{2.2 \times 10^{-11} \frac{mol(e^-)}{s}} = 9.6 \times 10^8\ s \approx 30\ y \tag{13}$$

This result is very much dependent on the specific ratio–mortar volume/embedded steel area–which in this case is 5.7 cm; when this value decreases or increases, t varies proportionally to it. Nevertheless, the calculation shows that the effect can prevail for a substantial portion of the design service life of a structure, even at the lower of the here investigated $Ca(NO_3)_2$ concentrations.

4.4 | Effect of Sodium Hydroxide (NaOH)

NaOH has been used for decades as an activator in the field of alkali-activated binders.[41] Regarding its influence on reinforcement corrosion, the alkali activator itself has never been taken into account as a possible influencing parameter of rebars corrosion because the admixture itself does not include particular corrosion enhancing ions. We suggest that the reason for the measured high corrosion rate increase (Table 2, Figure 2) can be traced to porosity and pore solution composition. While the porosity seems to be only slightly affected by the addition of NaOH (Figure 3), the results of pore solution composition (Table 1) show more interesting differences. A similar concentration of Ca and K was measured for CEM I, NB, and NB+1% NaOH mixes, the very high concentration of Na in the activated mix can easily be explained as coming from the activator itself. The concentration of S (SO_4^{2-}) increases by almost three times in the activated mix with respect to both CEM I and NB (Table 1). An increase of dissolved SO_4^{2-} in the pore solution, as consequent to the use of NaOH, is documented in literature.[42] This phenomenon has been explained as due to an increased solubility of sulphate bearing compounds, in order to maintain the electro neutrality of the solution and compensate for the Na^+ cations added to the system.[43] In cement chemistry, some studies have highlighted the impact of NaOH addition on the chemistry of alumino-sulphate phases: it was shown how it can affect both the reaction kinetics and the final products.[42-44] On the other hand, literature information on the impact of sulphate ions on rebars corrosion is almost nonexisting. Only two works were found, which studied the influence of $MgSO_4$ on steel corrosion, in simulated pore solution.[45-46] They found an increased corrosion rate as a consequence to the $MgSO_4$ addition. Also, sulphate ions (SO_4^{2-}) have been found to play a role in the atmospheric corrosion of steel, acting as a catalyst strongly accelerating the iron dissolution by interfering with the kinetics of the anodic reaction,[47-48] rather than by an electrochemical mechanism as in the case of nitrates (see section "Effect of Calcium Nitrate (Ca(NO3)2)").

4.5 | Combined Effect

When the two chemicals are added together (1% NaOH + 1% $Ca(NO_3)_2$), an additive effect seems to be present. The corrosion rate is higher than in both cases where 1% of one of the two species is used. Especially, it is interesting to notice the behavior between 95% RH and 99% RH: while the trend of the separated 1% NaOH and 1% $Ca(NO_3)_2$ is opposite, the use of both shows an averaged behavior (Figure 4). As discussed in the previous sections, the different chemicals contribute differently to the final corrosion rate. If the contributions are

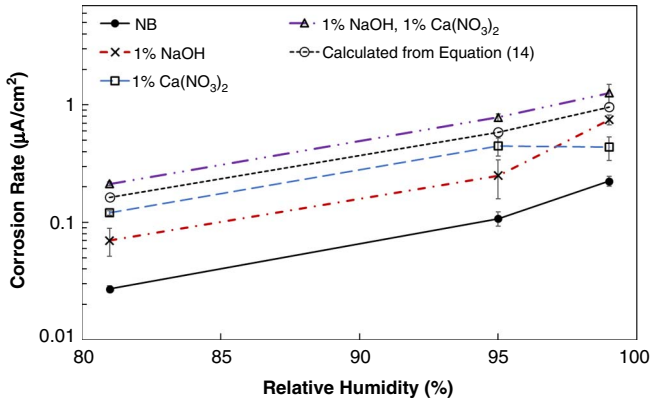

FIGURE 4. *Corrosion rates at different RH, for NB without and with addition of: 1% NaOH, 1% $Ca(NO_3)_2$, and 1% NaOH, $Ca(NO_3)_2$. In the figure is also represented the calculated corrosion rate, as by Equation (16).*

considered as additive, it should be possible to calculate the steel corrosion rate for the mix "NB + 1% NaOH, $Ca(NO_3)_2$" as

$$i_{corr,+1\%NaOH,Ca(NO_3)_2} = i_{corr,NB} + (i_{corr,+1\%NaOH} - i_{corr,NB}) + (i_{corr,+1\%Ca(NO_3)_2} - i_{corr,NB}) \quad (14)$$

The so-calculated combined effect leads to a slight underestimation of the measured corrosion rate (Figure 4), of a factor ca. 0.25, which is in the range of standard deviation of the corrosion rate measurements in this work.

The addition of compounds such as those here under study can lead to an increased electrical conductivity of the pore solution, which might affect the corrosion rate. The effect of the conductivity of the medium in the frame of carbonation-induced corrosion is somewhat controversial.[30-31] However, in the case of a microcell corrosion mechanism, as it is supposed to be for the corrosion process in carbonated concrete, it is believed that the mortar conductivity does not play a key role. This topic has been extensively considered in Stefanoni, et al.[31]

4.6 | Corrosion Rates in Mortar and in Simulated Solution

The corrosion rate of steel in carbonated mortar samples and in the simulated solutions is now compared. As it is not possible to refer to the absolute values of such different systems, the relative variation of corrosion rate depending on the relevant chemical species is considered. When the impact of sulphate ions is considered, where the concentration could be defined based on the pore solution composition (Table 1), the results in mortar and in solution are much more alike: In mortar "NB +1% NaOH," compared to "NB," the corrosion rate increased of a factor ca. 2.8, over all three exposure conditions tested. Accordingly, by adding to solution "R" 0.013 M SO_4^{2-} (solution "S"), a corrosion rate increase of a factor 2.5 was measured (Table 3), proving the sulphate effect on the steel corrosion rate. In the case of calcium nitrate in the mortar samples, the corrosion rate increase is very pronounced, showing an increase by a factor of ca. 4 when 1% is added, which becomes ca. 11 when 5% is added. Differently, the steel corrosion rate in the solution containing calcium nitrate (solution "N") is only ca. 1.6 times higher than in the reference solution "R" (Table 3). The reason can be found in the concentration of nitrate ions in the solution. As no information could be obtained on the actual nitrate concentration in the mortar pore solution, calcium nitrate has been added in order to have the same $[NO_3^-]$ concentration as for added sulphate ions in solution "S" (+0.013 M), with respect to the reference solution "R." In this way, the influence of the two species could be compared. However, the actual concentration of nitrate ions in mortar might be substantially higher, considering the very high solubility of $Ca(NO_3)_2$. It has to be noticed that, at equal species concentration, the sulphate effect is much more pronounced than the nitrate effect.

The combined addition of nitrates and sulphates in solutions led to a higher increase of the corrosion rate (Table 3), in agreement with the tests in mortars (Table 2). The increase of corrosion rate in solution "S-N," with respect to the reference solution "R," was of a factor ca. 3.5, which is again lower than the increase from mortar sample NB to 1% NaOH, $Ca(NO_3)_2$ (factor ca. 7, Table 2, Figure 2). This is explained, as above, because of a probable lower concentration of NO_3^-, with respect to the concentration in the mortar pore solution. Nevertheless, it can be noticed that, in the same way as in the mortars, the combined effect of nitrate and sulphate ions leads to a corrosion rate that is the result of the separate action of these chemicals.

The corrosion rate of steel in solution "S-N" may be calculated as:

$$i_{corr,S-N} = i_{corr,R} + (i_{corr,S} - i_{corr,R}) + (i_{corr,N} - i_{corr,R}) = 11.77\ \mu A/cm^2 \quad (15)$$

which is very close to the measured corrosion rate of 10.86 $\mu A/cm^2$.

CONCLUSIONS

➢ While the use of highly clinker replaced binders increases the corrosion rate of steel in carbonated concrete by a factor of approximately 2, the use of NaOH and $Ca(NO_3)_2$ as activating/accelerating admixtures was found to have a much more pronounced negative effect, that is, by factors in the range from 2 to 20. Moreover, the increasing effect on the corrosion rate was found to aggravate with increasing concentration as well as with combining the two chemicals. The tests in mortar and in solution were in good agreement and provided evidence that the impact of the admixtures can be mainly found in modifying the electrochemistry rather than through their influences on the mortar porosity. Electrochemical considerations indicated that the increase in corrosion rate is due to the introduction of an additional reduction reaction or by a catalyzing effect in the cases of $Ca(NO_3)_2$ and NaOH, respectively. An estimation revealed that at usual dosages, these adverse effects will prevail for a substantial portion of the design service life of a structure, as these species will not be consumed during decades. Based on this work, it is concluded that in applications that require the massive use of such compounds, alternative solutions need to be adopted to ensure corrosion resistant structures, such as the use of stainless steel rebars.

ACKNOWLEDGMENTS

Research supported by the Swiss National Foundation for Research (SNF) Project no. 154062 entitled "Formulation, use and durability of concrete with low clinker cements" is gratefully acknowledged. The authors would also like to thank Prof. Karen Scrivener and the LMC laboratory of EPFL Lausanne for the MIP measurements; Prof. Mette Geiker and Andres Belda Revert

from NTNU for the pore solution extraction; and Prof. Robert Flatt and Sara Mantellato from ETH Zurich for the ICP analysis. Prof. Pietro Lura from EMPA is acknowledged for the use of the carbonation chamber.

References

1. J.G. Olivier, J.A. Peters, G. Janssens-Maenhout, "Trends in Global CO_2 Emissions," 2015 report, PBL Netherlands Environmental Assessment Agency, The Hauge, 2015.
2. G. Oggioni, R. Riccardi, R. Toninelli, *Energ. Policy* 39 (2011): p. 2842-2854.
3. M. Schneider, M. Romer, M. Tschudin, H. Bolio, *Cem. Concr. Res.* 41 (2011): p. 642-650.
4. U.M. Angst, R.D. Hooton, J. Marchand, C.L. Page, R.J. Flatt, B. Elsener, C. Gehlen, J. Gulikers, *Mater. Corros.* 63 (2012): p. 1047-1051.
5. C. Shi, A.F. Jiménez, A. Palomo, *Cem. Concr. Res.* 41 (2011): p. 750-763.
6. T. Wangler, E. Lloret, L. Reiter, N. Hack, F. Gramazio, M. Kohler, M. Bernhard, B. Dillenburger, J. Buchli, N. Roussel, R. Flatt, *RILEM Technical Lett.* 1 (2016): p. 67-75.
7. D. Marchon, S. Kawashima, H. Bessaies-Bey, S. Mantellato, S. Ng, *Cem. Concr. Res.* 112 (2018): p. 96-100.
8. R. Feret, *Rev. Mater. Constr. Tr. Publications* (1939): p. 1-145.
9. D.M. Roy, *Cem. Concr. Res.* 29 (1999): p. 249-254.
10. J.L. Provis, *Cem. Concr. Res.* 114 (2018): p. 40-48.
11. H. Justnes, E.C. Nygaard, *Cem. Concr. Res.* 25 (1995): p. 1766-1774.
12. V. Dodson, "Set Accelerating Admixtures," in *Concrete Admixtures* (Boston, MA: Springer, 1990).
13. R. Myrdal, Accelerating Admixtures for Concrete. State of the art, COIN–Concrete Innovation Centre, Trondheim, 2007.
14. E. Lloret, A.R. Shahab, M. Linus, R.J. Flatt, F. Gramazio, M. Kohler, S. Langenberg, *Comput. Aided Des.* 60 (2015): p. 40-49.
15. R. Myrdal, Corrosion Inhibitors—State of the art, COIN–Concrete Innovation Centre, Trondheim, 2010.
16. T.A. Söylev, M.G. Richardson, *Constr. Build. Mater.* 22 (2008): p. 609-622.
17. H. Justnes, *Concrete* 44 (2010): p. 34-36.
18. A. Leemann, P. Nygaard, J. Kaufmann, R. Loser, *Cem. Concr. Compos.* 62 (2015): p. 33-43.
19. V.G. Papadakis, *Cem. Concr. Res.* 30 (2000): p. 291-299.
20. M. Stefanoni, U. Angst, B. Elsener, "Corrosion Challenges and Opportunities in Digital Fabrication of Reinforced Concrete," in *First RILEM International Conference on Concrete and Digital Fabrication–Digital Concrete 2018*, eds. T. Wangler, R.J. Flatt (Cham, Switzerland: Springer, 2019), p. 225.
21. S. Aggoun, M. Cheikh-Zouaoui, N. Chikh, R. Duval, *Constr. Build. Mater.* 22 (2008): p. 106-110.
22. M. Stefanoni, U. Angst, B. Elsener, "Innovative Sample Design for Corrosion Rate Measurement in Carbonated Concrete," in 11th Annual International Concrete Sustainability Conference (Washington, DC: 2016).
23. M. Stefanoni, U. Angst, B. Elsener, "A New Setup for Rapid Durability Screening of New Blended Cements," in 2nd Concrete Innovation Conference (Trosmo, Norway: 2017).
24. S.D. Wang, K.L. Scrivener, P.L. Pratt, *Cem. Concr. Res.* 24 (1994): p. 1033-1043.
25. C.F. Chang, J.W. Chen, *Cem. Concr. Res.* 36 (2006): p. 1760-1767.
26. R.G. Kelly, J.R. Scully, D. Shoesmith, R.G. Buchheit, "The Polarization Resistance Method for Determination of Instantaneous Corrosion Rates," *Electrochemical Techniques in Corrosion Science and Engineering* (Boca Raton, FL: CRC Press, 2002), p. 135-160.
27. C. Andrade, C. Alonso, *Mater. Struct.* 37 (2004): p. 623-643.
28. R.A. Buchanan, E.E. Stansbury, "Electrochemical Corrosion," in *Handbook of Environmental Degradation of Materials*, 2nd ed. (Norwich, NY: William Andrew, 2012), p. 87-125.
29. F. Caruso, S. Mantellato, M. Palacios, R.J. Flatt, *Cem. Concr. Res.* 91 (2017): p. 52-60.
30. M. Stefanoni, U. Angst, B. Elsener, *Cem. Concr. Res.* 103 (2018): p. 35-48.
31. M. Stefanoni, U. Angst, B. Elsener, *Sci. Rep.-UK*, 8 (2018): p. 7407.
32. C. Andrade, R. Buják, *Cem. Concr. Res.* 53 (2013): p. 59-67.
33. L. Bertolini, B. Elsener, P. Pedeferri, E. Redaelli, R. B. Polder, *Corrosion of Steel in Concrete: Prevention, Diagnosis, Repair* (New York, NY: John Wiley & Sons, 2013).
34. X. Fan, X. Guan, J. Ma, H. Ai, *J. Environ. Sci.* 21 (2009): p. 1028-1035.
35. G.C. Yang, H.L. Lee, *Water Res.* 39 (2005): p. 884-894.
36. M. Balonis, M. Medala, F.P. Glasser, *Adv. Cem. Res.* 23 (2011): p. 129-143.
37. B. Morgan, O. Lahav, *Chemosphere* 68 (2007): p. 2080-2084.
38. M. Stefanoni, U. Angst, B. Elsener, *RILEM Tech. Lett.* 3 (2018): p. 8-16.
39. T. Suzuki, M. Moribe, Y. Oyama, M. Niinae, *Chem. Eng. J.* 183 (2012): p. 271-277.
40. J. Van Muylder, M. Pourbaix, *Atlas d'équilibres électrochimiques* (Paris, France: 1963).
41. F. Pacheco-Torgal, J. Castro-Gomes, S. Jalali, *Constr. Build. Mater.* 22 (2008): p. 1305-1314.
42. S.J. Way, A. Shayan, *Cem. Concr. Res.* 19 (1989): p. 759-769.
43. D. Damidot, F.P. Glasser, *Cem. Concr. Res.* 23 (1993): p. 221-238.
44. B.A. Clark, P.W. Brown, *J. Am. Ceram. Soc.* 82 (1999): p. 2900-2905.
45. L. Hachani, J. Carpio, C. Fiaud, A. Raharinaivo, E. Triki, *Cem. Concr. Res.* 22 (1992): p. 56-66.
46. L. Mammoliti, C.M. Hansson, *ACI Mater. J.* 102 (2005): p. 279-285.
47. J.R. Walton, J.B. Johnson, G.C. Wood, *Brit. Corros. J.* 17 (1982): p. 65-70.
48. K. Bartoň, Ž. Bartoňová, *Mater. Corros.* 20 (1969): p. 216-221.